SPECIAL ISSUE REVIEW

Exendin-4 analogs in insulinoma theranostics

Tom.J.P. Jansen[1] (iD) | Sanne.A.M. van Lith[1] | Marti Boss[1] | Maarten Brom[1] | Lieke Joosten[1] |
Martin Béhé[2] | Mijke Buitinga[1,3] | Martin Gotthardt[1]

[1] Department of Radiology and Nuclear Medicine, Radboudumc, Nijmegen, The Netherlands

[2] Center for Radiopharmaceutical Sciences ETH-PSI-USZ, Paul Scherrer Institute, Villigen, Switzerland

[3] Department of Clinical and Experimental Medicine, KU Leuven, Leuven, Belgium

Correspondence
Martin Gotthardt, Department of Radiology and Nuclear Medicine, Radboudumc, Nijmegen, The Netherlands.
Email: martin.gotthardt@radboudumc.nl

Insulinomas are neuroendocrine tumors arising from the pancreatic beta cells. Currently, surgical resection is the therapy of choice, and therefore, preoperative localization of insulinomas is essential. Nearly all insulinomas show overexpression of the glucagon-like peptide-1 receptor (GLP-1R), and therefore, radiolabeled GLP-1 peptide analog exendin-4 can be used for diagnosis and preoperative localization with nuclear imaging. Here, we present an overview of the development and clinical implementation of exendin-4–based tracers for single-photon emission computed tomography (SPECT) and positron emission tomography (PET) imaging of insulinomas, and we address the potential use of this molecule for optical imaging. At last, we discuss the possibilities and pitfalls of the use of exendin-4–based tracers for therapeutic applications such as peptide receptor radionuclide therapy (PRRT) or targeted photodynamic therapy (tPDT), giving a future outlook on the use of exendin-4 in insulinoma theranostics.

KEYWORDS
exendin-4, GLP-1 receptor, insulinoma, peptide receptor radionuclide therapy (PRRT), positron emission tomography (PET), single-photon emission computed tomography (SPECT), targeted photodynamic therapy (tPDT), theranostics

1 | CLINICAL CHARACTERISTICS AND THERAPY OF INSULINOMA

Insulinoma is a subtype of pancreatic neuroendocrine tumors (pNETs) that arises from the insulin-producing beta cells in the islets of Langerhans. Although the majority of insulinomas are benign (90%), symptoms due to the excessive insulin secretion by the tumor cells can be severe and have a major impact on the patient's quality

of life. Symptoms include hypoglycemia, impaired consciousness, disturbances of speech and vision, seizures, and sensorimotor function impairment. Furthermore, behavioral changes, personality changes, and weight gain due to continuous eating may occur.[1,2] Insulinoma is currently diagnosed biochemically by measuring plasma glucose, insulin, C-peptide, and proinsulin during a 12- to 72-hour period of fasting, showing low glucose levels with inappropriately high insulin levels. Treatment options include surgical resection, radiofrequency ablation, alcohol ablation, embolization, chemotherapy, medication, and peptide receptor radionuclide therapy (PRRT).[3-7] Since surgical resection is the only curative treatment

option for insulinoma, patients are eligible for surgery once the clinical diagnosis has been made and the tumor has been localized using preoperative imaging.

2 | PREOPERATIVE IMAGING OF INSULINOMA

Preoperative imaging is essential to localize the lesion, plan the surgical procedure (eg, enucleation of the lesion or partial pancreatic resection), and determine whether laparoscopic resection is feasible. Typically, the size of insulinomas is small (82% < 2 cm and 47% < 1 cm).[8] This hampers detection by noninvasive imaging methods such as ultrasound (US), computed tomography (CT), and magnetic resonance imaging (MRI), which have mean sensitivities of only 32.6%, 43.9%, and 53.3%, respectively.[3] Methods with higher sensitivity are angiography with intraarterial calcium stimulation and venous sampling (ASVS), with a sensitivity of 85%, and endoscopic ultrasound (EUS), with a sensitivity of 74.8%. However, shortcomings of these methods are their invasive nature, with concomitant risk of complications, and that they are operator dependent.[3,9-12] Since the majority of neuroendocrine tumors (NETs) express somatostatin receptors (SSTRs) at high levels, somatostatin receptor scintigraphy (SRS) with the radiolabeled peptide octreotide (binding SSTR subtypes 2 and 5) and its derivatives is a very efficient detection method.[13,14] In benign insulinoma however, the receptor density of SSTR subtypes 2 and 5 is low, and therefore, sensitivity of SRS is relatively poor (<50%).[15,16] Recently, the use of SSTR positron emission tomography (PET) tracers [Ga^{68}]Ga-DOTA-TOC and [Ga^{68}]Ga-DOTA-TATE for detection of insulinomas resulted in improved sensitivity of 87%,[17,18] which is mainly due to the better spatial resolution and sensitivity of PET when compared with scintigraphy and due to better affinity of the PET tracers for SSTRs. In contrast to low SSTR expression, benign insulinomas do express high levels of the glucagon-like peptide-1 receptor (GLP-1R) in nearly 100% of cases and are therefore suitable candidates for single-photon emission computed tomography (SPECT) or PET imaging with glucagon-like peptide-1 (GLP-1) analogs.[19] Iodinated GLP-1(7-36) was the first tracer to be investigated as a possible tool for insulinoma detection targeting the GLP-1R, and it showed specific tumor targeting in preclinical models for insulinoma.[20] However, low peptide stability of GLP-1 in blood and rapid deinodination limits clinical use, and therefore, multiple radiolabeled tracers of the natural GLP-1 analog exendin-4 have been developed. Exendin-4 is isolated from the saliva of the Gila monster (*Heloderma suspectum*),[21] and since the dipeptidyl peptidase-IV enzymatic cleavage site is not present in this peptide, it is resistant to degradation in serum, resulting in an increased biological half-life of ≥20 minutes compared with GLP-1 (≤2 min).[22]

In this review, we will give an overview of development of exendin-4–based tracers and their clinical implementation for insulinoma imaging. We will also address some pitfalls of exendin-4–based imaging. Furthermore, we will discuss on the future outlook of the use of exendin-4 in insulinoma theranostics (for an overview, see Figure 1).

3 | IMAGING OF INSULINOMA WITH EXENDIN-4–BASED TRACERS

3.1 | Tracer development and clinical implementation

The first exendin-4–based imaging tracer that was developed is the diethylenetriaminepentaacetic acid (DTPA) conjugate [Lys^{40}(Ahx-DTPA-[^{111}In]In)NH$_2$]-exendin-4.[23,24] This tracer showed high receptor affinity and remarkably high tumor uptake (287 ± 62 %IA/g) in the Rip1Tag2 mouse model[24] (for an overview of exendin-based SPECT tracers and characteristics, see Tables 1 and 2). [Lys^{40}(Ahx-DOTA-[^{111}In]In)NH$_2$]-exendin-4 was also the first tracer to be used in clinical diagnosis of insulinoma.[25] In a prospective pilot study, whole-body planar and SPECT/CT imaging with this tracer successfully detected an insulinoma in all six patients that presented with biochemically proven endogenous hyperinsulinemic hypoglycemia, whereas it was missed in five out of six patients with MRI and in two out of six patients with endosonography. In a second prospective study including 30 patients, [Lys^{40}(Ahx-DTPA-[^{111}In]In)NH$_2$]-exendin-4 SPECT/CT was proven to be a more sensitive method for insulinoma detection than conventional imaging (CT or MRI) (sensitivity of 95% vs. 47%, respectively).[26]

The use of indium-111 has drawbacks since it is costly and carries a relatively high radiation burden for the patient. Technetium-99m can be used to overcome these drawbacks because of its low energy and shorter half-life. To this end, [Lys^{40}(Ahx-HYNIC-[^{99m}Tc]Tc)NH$_2$]-exendin-4 was developed, and tumor and organ uptake in the Rip1Tag2 mice was lower compared with [Lys^{40}(Ahx-DTPA-[^{111}In]In)NH$_2$]-exendin-4,[27] which could be explained by less efficient internalization of the ^{99m}Tc-labeled tracer. Although the tumor uptake is lower, small lesions (1.0-3.2 mm in diameter) could still be detected with SPECT. [Lys^{40}(Ahx-HYNIC-[^{99m}Tc]Tc/EDDA)NH$_2$]-exendin-4 was injected in eight patients with clinical and biochemical signs of insulinoma, and in all patients, focal uptake of the tracer was found. In six out of eight patients, surgical excision of the lesion was performed, and these lesions were insulin-producing G1 NETs as confirmed by
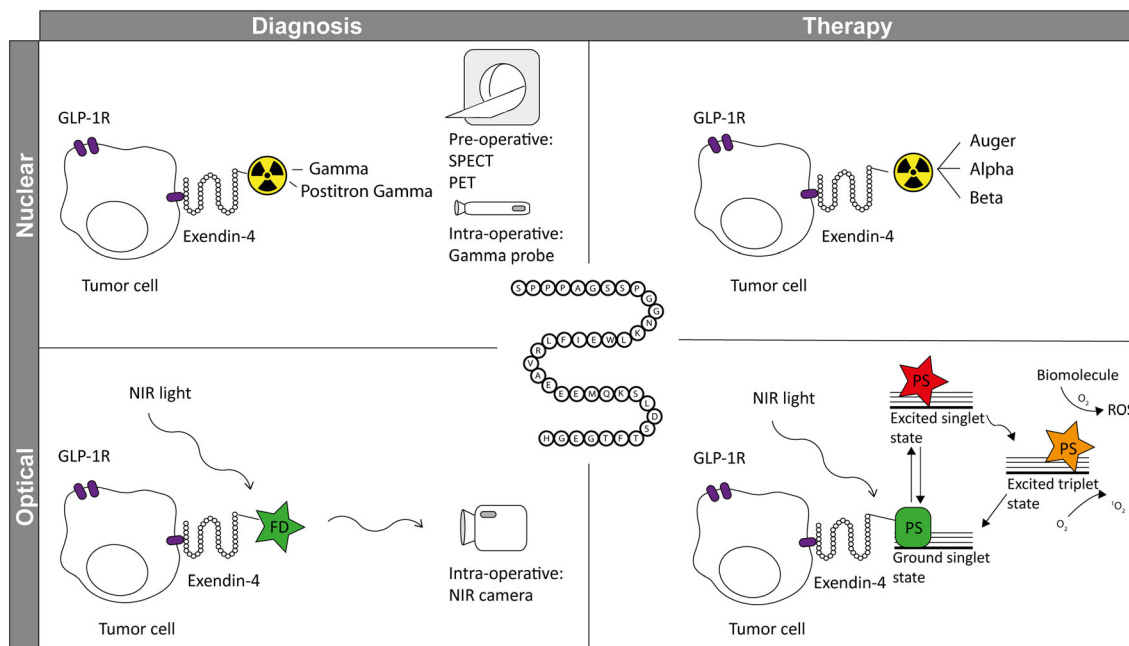
FIGURE 1 Exendin-4 in theranostics of insulinoma. Exendin-4 can be used for diagnosis of GLP-1 receptor (GLP-1R) expressing tumor cells upon conjugation with 1) a radionuclide and preoperative SPECT or PET imaging or intraoperative detection with a gamma probe or 2) a fluorescent dye (FD) and intraoperative imaging with a near-infrared (NIR) light camera. The same molecule can be used for therapy of GLP-1R expressing tumor cells upon conjugation with 1) a therapeutic radionuclide for peptide receptor radionuclide therapy (PRRT) and 2) a photosensitizer (PS) for targeted photodynamic therapy (tPDT).

histopathology.[28] In a second study, 40 patients experiencing episodes of hypoglycemia with no signs of an insulinoma based on conventional imaging methods were included. In 28 of these patients, the [Lys^{40}(Ahx-HYNIC-[^{99m}Tc]Tc/EDDA)NH$_2$]-exendin-4 scan was positive, and in 18 patients, the presence of an insulinoma was confirmed histopathologically. The other 10 patients could not undergo surgery.[29]

PET imaging has a number of advantages over SPECT imaging, such as higher sensitivity so that lower amounts of a tracer molecule can be detected, better spatial resolution, and more accurate quantification. Therefore, multiple exendin-4–based PET tracers have been developed (for an overview of developed PET tracers and their characteristics, see Tables 3 and 4). Fluorine-18 is a favorable radionuclide for PET imaging because of the low positron emission energy, which provides a short tissue range and thus the potential for achieving a high resolution. As the conditions typically required for ^{18}F-fluorination are very harsh (eg, high temperatures and strong bases), prosthetic groups that can be labeled and conjugated to functional moieties of the exendin-4 have been developed.[30-35] Interestingly, kidney uptake of these tracers is high at first, but clearance from the kidneys is more rapid compared with radiometal-labeled exendin. To overcome the time-consuming synthesis of prosthetic groups, other strategies such as aluminum complexation were applied and showed high tracer uptake by the tumor as well.[36-38]

The use of generator-produced positron emitting gallium-68 makes tracers affordable, and it eliminates the need for a cyclotron on site. Lys^{40}(Ahx-DOTA-[^{68}Ga]Ga)NH2]-exendin-4 showed high tumor uptake (205 ± 59 %IA/g) 4 hours after injection in Rip1Tag2 mice.[27] The [^{68}Ga]Ga-DO3A-VS-Cys40-exendin-4 tracer could be labeled with six times higher specific activity compared with Lys^{40}(Ahx-DOTA-[^{68}Ga]Ga)NH2]-exendin-4, thereby enabling injection of lower peptide dose, and this tracer also showed good tumor uptake in INS-1 xenografts.[39] During the recent years, multiple case reports have been published in which ^{68}Ga-labeled exendin-4 tracers enabled successful detection of insulinomas with PET/CT, while other imaging methods were negative[11,40-44] (for an overview of clinical PET tracers, see Table 4). Antwi et al performed the first pilot study directly comparing [^{111}In]In-DOTA-exendin-4 SPECT/CT with [^{68}Ga]Ga-DOTA-exendin-4 for detection of insulinoma in five patients. In the four patients that were operated on, better spatial resolution and better tumor-to-background ratios allowed for detection of four out of four lesions with [^{68}Ga]Ga-DOTA-exendin-4, while [^{111}In]In-DOTA-exendin-4 detected two out of four lesions.[45] One patient refused surgery, despite a positive [^{68}Ga]Ga-DOTA-exendin-4 scan. In a prospective cohort study, 52 patients with hyperinsulinemic hypoglycemia were included, and various imaging modalities including [^{68}Ga]Ga-NOTA-exendin-4 PET/CT were applied. Forty-three patients that

TABLE 1 Overview of preclinical SPECT tracers and their characteristics

Author + Year	Compound	Tumor Model	Peptide Dose	Activity Dose	Tumor Uptake	Kidney Uptake
Indium-111						
Wild et al. 2006	[Lys^{40}(Ahx-[^{111}In]In-DTPA)NH2]exendin-4	RipTag2 and C57BL/6J RipTag2	10 ng (BD) 50 pmol (Im)	185-370 kBq (BD) 37 MBq (Im)	287 ± 62 %IA/g (4 h)	209 ± 35 %IA/g (4 h)
Wild et al. 2010	[Lys^{40}(Ahx-DTPA-[^{111}In]In)NH2]exendin-4	RipTag2	10 pmol	70-110 kBq	213 ± 75 %IA/g (4 h)	243 ± 17 %IA/g (4 h)
Brom et al. 2012	[Lys^{40}(Ahx-[^{111}In]In-DTPA)NH2]exendin-3	INS-1	20 pmol	370 kBq	25.0 ± 6.0 %ID/g (30 min) 26.5 ± 8.9 %ID/g (4 h)	150.7 ± 14.9 %ID/g (30 min) 188.8 ± 14.4 %ID/g (4 h)
Brom et al. 2012	[Lys^{40}(Ahx-[^{111}In]In-DTPA)NH2]exendin-4	INS-1	20 pmol	370 kBq	30.7 ± 6.1 %ID/g (30 min) 41.9 ± 7.2 %ID/g (4 h)	150.9 ± 9.6 %ID/g (30 min) 173.6 ± 24.3 %ID/g (4 h)
Brom et al. 2012	[Lys^{40}(Ahx-[^{111}In]In-DTPA)NH2]exendin(9-39)	INS-1	20 pmol	370 kBq	3.2 ± 0.7 %ID/g (30 min) 0.71 ± 0.2 %ID/g (4 h)	65.7 ± 6.1 %ID/g (30 min) 70.7 ± 4.0 %ID/g (4 h)
Bauman et al. 2015	[Lys^{40}-(AHX-DTPA-[^{111}In]In)NH$_2$]exendin-4	RIN-m5f	10 pmol, 52 ng	385 kBq	14.74 ± 5.91 %ID/g (1 h) 15.56 ± 5.32 %ID/g (4 h) 9.31 ± 2.35 %ID/g (24 h) 3.47 ± 0.52 %ID/g (48 h)	152.70 ± 24.86 %ID/g (1 h) 178.41 ± 33.66 %ID/g (4 h) 144.09 ± 20.94 %ID/g (24 h) 84.80 ± 19.26 %ID/g (48 h)
Kimura et al. 2017	[Lys^{12}([^{111}In]In-BnDTPA)]exendin-9-39	INS-1	1.5 ng 790 ng	37 kBq/100 μL (BD) 19.9 MBq/220 μL (Im)	7.83 ± 1.86 %ID/g (30 min) 1.87 ± 0.52 %ID/g (4 h) –	193.6 ± 15.1 %ID/g (30 min) 180.9 ± 52.7 %ID/g (4 h) –
Technetium-99m						
Wild et al. 2010	[Lys^{40}(Ahx-HYNIC-[^{99m}Tc]Tc/EDDA)NH2]exendin-4	RipTag2	10 pmol (BD) –	70-110 kBq (BD) 37 MBq (Im)	67 ± 13 %IA/g (30 min) 93.1 ± 19.9 %IA/g (4 h) –	63 ± 10 %IA/g (30 min) 60 ± 12 %IA/g (4 h) –
Medina-Garcia et al. 2015	[Lys^{27}([^{99m}Tc]Tc-EDDA/HYNIC)]exendin(9-39)	AR42J induced	–	1.85 MBq	2.41 ± 0.38 %ID/g (2 h)	95.01 ± 1.95 %ID/g (2 h)

Abbreviations: BD, biodistribution; Im, imaging; SPECT, single-photon emission computed tomography.

were operated on and had histopathologically proven insulinoma were included for analysis. [^{68}Ga]Ga-NOTA-exendin-4 PET/CT showed a very high sensitivity of 97.7%, in contrast to 74.4% for CT, 56% for MRI, 84% for EUS, and 19.5% for [^{99m}Tc]Tc-HYNIC-TOC SPECT/CT.[43]

In a prospective crossover imaging study with GLP-1R PET/CT, GLP-1R SPECT/CT, and 3T MRI, 52 patients with biochemically proven endogenous hyperinsulinemic hypoglycemia were included. For each patient, a [^{68}Ga]Ga-DOTA-exendin-4 PET/CT scan,

TABLE 2 Overview of clinical single-photon emission computed tomography (SPECT) tracers and study outcomes

Author + Year	Compound	Patients	Peptide Dose	Activity Dose	Results	Adverse Events
Indium-111						
Christ et al. 2009	[Lys^{40}(AHX-DOTA-[In^{111}]In)NH$_2$] exendin-4	6	30 µg	82-97 MBq	In all six patients, the insulinoma was correctly localized.	- Decrease in blood glucose levels 0.3-2.4 mmol/L, glucose infusion needed in three patients - Vomiting (n = 1)
Wild et al. 2011	[Lys^{40}(AHX-DTPA-[In^{111}]In)NH$_2$] exendin-4	11	10 ± 2 µg	108-136 MBq	Uptake in four patients was observed with malignant insulinomas that were expressing the GLP-1R.	- Decrease in blood glucose levels 1.1-3.3 mmol/L in GLP-1R–positive patients, 0.5-0.6 mmol/L in GLP-1R–negative patients
Christ et al. 2013	[Lys^{40}(AHX-DTPA-[In^{111}]In)NH$_2$] exendin-4	30	8-14 µg	80-128 MBq	95% (75-100) sensitivity 20% (2-64) specificity 83% (62-94) positive predictive value	- Decrease in blood glucose levels 0-2.6 mmol/L, glucose infusion needed in 20 patients
Antwi et al. 2015	[Nle$_{14}$, Lys$_{40}$(Ahx-DOTA-[^{111}In]In)NH$_2$] exendin-4]	5	10.5-14.4 µg	79.2 ± 9.3 MBq (66-90 MBq)	In four out of five patients that had surgery, an insulinoma was found in two of four patients.	- Prophylactic glucose infusion was given before the injection - Nausea (n = 2) and vomiting (n = 2)
Antwi et al. 2018	[^{111}In]In-DOTA-exendin-4	52	11.0-16.9 µg	87.5 ± 10.7 MBq (52-111 MBq)	Sensitivity 68.5% (59.0-77.0)	- No hypoglycemia due to continuous infusion of glucose - Nausea (n = 27) and vomiting (n = 23)
Fluorine-18						
Sowa-Staszczak et al. 2013	[Lys^{40}(Ahx-HYNIC-[^{99m}Tc]Tc/EDDA)NH$_2$]-exendin-4	11	–	740 MBq (mean)	Focal uptake in all eight cases with suspicion of benign insulinomas was observed. In six of the eight patients, surgery was performed and the presence of an insulinoma was confirmed.	- Most patients with benign insulinoma needed glucose infusion
Sowa-Staszczak et al. 2016	[Lys^{40}(Ahx-HYNIC-[^{99m}Tc]Tc/EDDA)NH$_2$]-exendin-4	40	–	740 MBq (mean)	Uptake was seen in 28 patients. In 18 out of 28 cases, insulinomas were identified histopathologically.	- All patients with suspected benign insulinoma needed glucose infusion

[^{111}In]In-DOTA-exendin-4 SPECT/CT scans (4 and 72 h), and an MRI scan were performed. In 38 out of 52 patients, histological confirmation could be obtained, and this resulted in sensitivities of 94.6%, 68.5%, and 69.4% for [^{68}Ga]Ga-DOTA-exendin-4, [^{111}In]In-DOTA-exendin-4, and MRI, respectively.[46] Although spatial resolution of PET/CT is better compared with SPECT/CT, small lesions can still be missed as is illustrated by the only false-negative PET/CT finding of a 5 × 5 × 10 mm insulinoma in this study.

High kidney accumulation of exendin-4–based tracers can complicate imaging applications, since the tail of the pancreas is located close to the kidney. For both indium-111 and technetium-99m exendin-based tracers, tumor-to-kidney ratios do increase over time, and therefore, authors suggest that additional late scans should be made

TABLE 3 Overview of preclinical PET tracers and their characteristics

Author + Year	Compound	Tumor Model	Peptide Dose	Activity Dose	Tumor Uptake	Kidney Uptake
Gallium-68						
Wild et al. 2010	[Lys^{40}(Ahx-DOTA-[^{68}Ga]Ga)NH2]exendin-4	RipTag2	10 pmol	70-110 kBq	185 $\pm$ 33 %IA/g (30 min) 205 $\pm$ 59 %IA/g (4 h)	255 $\pm$ 14 %IA/g 202 $\pm$ 34 %IA/g
Selvaraju et al. 2014	[^{68}Ga]Ga-DO3A-VS-Cys^{40}-Exendin-4	INS-1 xenografts	2.5 µg/kg	0.6 $\pm$ 0.1 MBq	Tumor-to-muscle ratio 44.8 (80 min)	–
Bauman et al. 2015	[Lys^{40}-(AHX-DFO-[^{68}Ga]Ga)NH$_2$]exendin-4	RIN-m5f xenografts	10 pmol, 52 ng	385 kBq	32.48 $\pm$ 8.26 %ID/g (1 h)	141.51 $\pm$ 25.14 %ID/g (1 h)
Rylova et al. 2016	[Nle^{14},Lys^{40}(Ahx-DOTA-[^{68}Ga]Ga)NH$_2$]exendin-4	INS-1 xenografts	100 pmol (BD) 100 pmol (Im)	0.4-0.9 MBq (BD) 0.4-0.9 MBq (Im)	40.2 $\pm$ 8.2 %IA/g (1 h) –	235.8 $\pm$ 17.0 %IA/g (1 h) –
Rylova et al. 2016	[Lys^{27}(Ahx-DOTA-[^{68}Ga]Ga]exendin(9-39)NH$_2$	INS-1 xenografts	100 pmol (BD)	0.4-0.9 MBq (BD)	–	113.8 $\pm$ 23.8 %IA/g (1 h)
Rylova et al. 2016	[Lys^{27}(NODAGA-[^{68}Ga]Ga]exendin(9-39)NH$_2$	INS-1 xenografts	100 pmol (BD)	0.4-0.9 MBq (BD)	0.7 $\pm$ 0.2 %IA/g (1 h)	101.0 $\pm$ 21.0 %IA/g (1 h)
Rylova et al. 2016	[Lys^{40}(NODAGA-[^{68}Ga]Ga)NH$_2$]exendin(9-39)	INS-1 xenografts	100 pmol (BD) 100 pmol (Im)	0.4-0.9 MBq (BD) 0.4-0.9 MBq (Im)	2.2 $\pm$ 0.2 %IA/g (1 h) –	78.4 $\pm$ 8.5 %IA/g (1 h) –
Läppchen et al. 2017	[Nle^{14},Lys^{40}(Ahx-DOTA-[^{68}Ga]Ga)NH$_2$]exendin-4	INS-1 xenografts	10 pmol (BD)	–	58.3 $\pm$ 15.6 %IA/g (1 h)	201.3 $\pm$ 30.6 %IA/g (1 h)
Fluorine-18						
Kiesewetter et al. 2012	[^{18}F]FBEM-[Cys^{40}]exendin-4	INS-1 xenografts	0.5-1 µg (BD) 0.5-1 µg (Im)	3.44 $\pm$ 0.26 MBq (BD) 3.44 $\pm$ 0.26 MBq (Im)	– 25.25 $\pm$ 3.39 %ID/g (1 h)	Tumor-to-kidney ratio 7.4 (2 h) Tumor-to-kidney ratio 4.94 (2 h)
Kiesewetter et al. 2012	[^{18}F]FBEM-[Cys^{0}]-exendin-4	INS-1 xenografts	0.5-1 µg (BD) 0.5-1 µg (Im)	3.44 $\pm$ 0.26 MBq (BD) 3.44 $\pm$ 0.26 MBq (Im)	– 7.2 $\pm$ 1.26 %ID/g (1 h)	Tumor-to-kidney ratio 0.48 (2 h) Tumor-to-kidney ratio 0.74 (2 h)
Kiesewetter et al. 2012	[^{18}F]AlF-NOTA-MAL-Cys^{40}-exendin-4	INS-1 xenografts	300 pmol (BD) 300 pmol (Im)	3.44 $\pm$ 0.26 MBq (BD) 3.44 $\pm$ 0.26 MBq (Im)	17.9 $\pm$ 1.4 %ID/g (1 h) 15.7 $\pm$ 1.4 %ID/g (30 min) 14.6 $\pm$ 1.3 %ID/g (1 h)	– 79.3 $\pm$ 3.7 %ID/g (30 min) 74.7 $\pm$ 6.2 %ID/g (1 h)
Wu et al. 2013	[^{18}F]FB-exendin-4	RIN-m5f xenografts	40 µg (BD) 40 µg (Im)	3.7 MBq (BD) 3.7 MBq (Im)	0.15 %ID/g (2 h) –	0.27 %ID/g (2 h) –
Yue et al. 2013	[^{18}F]FPenM-[cys^{40}]-exendin-4	INS-1 xenografts	– –	3.7 MBq (Im) 3.7 MBq (BD)	21.30 $\pm$ 4.55 %ID/g (30 min) 20.32 $\pm$ 4.36 %ID/g (1 h) – 33.21 $\pm$ 4.79 %ID/g (1 h)	34.41 $\pm$ 4.59 %ID/g (30 min) 11.30 $\pm$ 2.41 %ID/g (1 h) 33 %ID/g (30 min) 11 %ID/g (1 h)
Xu et al. 2014	[^{18}F]FBEM-Cys^{39}-exendin-4	INS-1 xenografts	106 pmol (BD) 21 pmol (Im)	0.74 MBq (BD) 3.7 MBq (Im)	12.85 $\pm$ 2.21 %ID/g (30 min)	29.64 $\pm$ 3.47 %ID/g (30 min)

TABLE 3 (Continued)

Author + Year	Compound	Tumor Model	Peptide Dose	Activity Dose	Tumor Uptake	Kidney Uptake
					10.06 ± 1.93 %ID/g (2 h)	12.43 ± 0.75 %ID/g (2 h)
					10.71 ± 1.46 %ID/g (30 min)	21.27 ± 4.10 %ID/g (30 min)
					9.19 ± 0.86 %ID/g (2 h)	11.62 ± 2.08 %ID/g (2 h)
Xu et al. 2015	[^{18}F]AlF-NOTA-MAL-Cys39-exendin-4	INS-1 xenografts	128 pmol (BD) 638 pmol (Im)	0.74 MBq (BD) 3.7 MBq (Im)	8.68 ± 0.46 %ID/g (30 min) 7.59 ± 0.60 %ID/g (1 h) 9.15 ± 1.6 %ID/g (30 min) 7.74 ± 0.87 %ID/g (1 h)	86.19 ± 4.87 %ID/g (30 min) 95.91 ± 9.20 %ID/g (1 h) 75.12 ± 4.35 %ID/g (30 min) 85.32 ± 5.89 %ID/g (1 h)
Dialer et al. 2018	[^{18}F]F-2	CHL-GLP-1R xenografts	1.3 pmol, 5.9 ng (BD) 1.3 nmol (Im)	200 kBq (BD) 13 MBq (Im)	15 ± 7 %ID/g (30 min) 14 ± 7 %ID/g (1 h) 13 ± 10 %ID/g (2 h) SUV_{tumor} of 2.2 (2 h)	33.3 ± 2.4 %ID/g (30 min) 49 ± 18 %ID/g (1 h) 39 ± 12 %ID/g (2 h) $SUV_{kidneys}$ of 4.1 (2 h)
Zirconium-89						
Bauman et al. 2015	[Lys^{40}-(AHX-DFO-[^{89}Zr]Zr)NH$_2$]exendin-4	RIN-m5f xenografts	10 pmol, 52 ng	385 kBq	13.46 ± 0.79 %ID/g (1 h) 11.73 ± 3.17 %ID/g (4 h) 8.23 ± 1.61 %ID/g (24 h) 3.1 ± 0.17 %ID/g (48 h)	216.89 ± 56.22 %ID/g (1 h) 188.25 ± 52.22 %ID/g (4 h) 169.12 ± 44.87 %ID/g (24 h) 144.27 ± 1.68 %ID/g (48 h)
Iodine-125						
Rylova et al. 2016	[[^{125}I]I-BH-Lys^{27}]exendin(9-39)NH$_2$	INS-1 xenografts	–	0.037 MBq (BD)	42.5 ± 8.1 %IA/g (1 h) 19.8 ± 4.3 %IA/g (4 h)	12.1 ± 1.4 %IA/g (1 h) 4.2 ± 0.7 %IA/g (4 h)
Läppchen et al. 2017	[Nle^{14},[^{125}I]I-Tyr^{40}-NH$_2$]exendin-4	INS-1 xenografts	0.5 pmol (BD) –	40 KBq (BD) 2.5-3.0 MBq (Im)	72.8 ± 12.2 %IA/g (1 h) 22.4 ± 2.9 %IA/g (4 h) 3.7 ± 2.5 %IA/g (24 h)	7.5 ± 0.7 %IA/g (1 h) 3.2 ± 0.3 %IA/g (4 h) 0.2 ± 0.0 %IA/g (24 h)
Läppchen et al. 2017	[Nle^{14},[^{125}I]I-Tyr^{40}-NH$_2$]exendin(9-39)	INS-1 xenografts	0.5 pmol (BD)	40 KBq (BD)	12.7 ± 4.1 %IA/g (1 h) 1.9 ± 0.5 %IA/g (4 h)	7.6 ± 1.2 %IA/g (1 h) 2.0 ± 0.3 %IA/g (4 h)

Abbreviations: BD, biodistribution; Im, imaging; PET, positron emission tomography.

in case of negative scans early after injection,[28,29,47,48] as has been suggested for longer-lived positron-emitting radionuclides such as zirconium-89 as well.[49] The use of radioiodinated exendin-based tracers should also be considered to reduce renal accumulation.[50,51]

3.2 | Imaging of benign versus malignant insulinoma

Nearly all benign insulinomas express GLP-1R whereas expression of SSTR is low or not present. This while

TABLE 4 Overview of clinical positron emission tomography (PET) tracers and study outcomes

Author + Year	Compound	Patients	Peptide Dose	Activity Dose	Results	Adverse Events
Gallium-68						
Eriksson et al. 2014	[^{68}Ga]Ga-DO3A-VS-Cys^{40}-Exendin-4	1	0.17 µg/kg	0.88 MBq/kg	Detection of liver and lymph node metastases	–
Antwi et al. 2015	[Nle$_{14}$, Lys$_{40}$(Ahx-DOTA-[^{68}Ga]Ga)NH$_2$] exendin-4]	5	12.0-15.3 µg	79.8 ± 3.9 MBq (76-97 MBq)	In four out of 5 patients that had surgery, an insulinoma was found in four of four patients	- Prophylactic glucose infusion was given before the injection - Nausea (n = 1)
Luo et al. 2015	[^{68}Ga]Ga-NOTA-exendin-4	1	–	–	Detection of insulinoma in the pancreas tail (SUV$_{max}$ of 20.7)	–
Cuthbertson et al. 2015	[^{68}Ga]Ga-NOTA-exendin-4	1	–	–	Detection of insulinoma	–
Luo et al. 2016	[^{68}Ga]Ga-NOTA-exendin-4	1	–	51.8 MBq	Detection of insulinoma in the pancreas tail (SUV$_{mean}$ of 20.0 and SUV$_{max}$ of 52.9)	–
Luo et al. 2016	[^{68}Ga]Ga-NOTA-MAL-Cys^{40}-exendin-4	52	7-25 µg	18.5-185 MBq	In 43 of 52 patients, surgery was performed. In 42 patients, an insulinoma was found (sensitivity of 97.7%)	- No hypoglycemia was observed because of continuous infusion of glucose - Nausea (n = 2) - Vomiting (n = 2)
Luo et al. 2017	[^{68}Ga]Ga-exendin-4	1	–	–	Detection of a lesion that was ablated with ethanol ablation (SUV$_{mean}$ of 5.7 and SUV$_{max}$ of 10.8)	–
Bongetti et al. 2018	[^{68}Ga]Ga-DOTA-exendin-4	1	–	–	The ^{68}Ga-DOTA-exendin-4 was suggestive of nesidioblastosis; however, an insulinoma as identified with SACST and EUS was missed, noting that the insulinoma was negative for GLP-1R	–
Parihar et al. 2018	[^{68}Ga]Ga-DOTA-exendin-4	1	–	–	Detection of insulinoma (SUV$_{max}$ of 21)	–
Antwi et al. 2018	[^{68}Ga]Ga-DOTA-exendin-4	52	11.6-23.8 µg	82.4 ± 14.9 MBq (43-106 MBq)	Sensitivity 94.6% (88.6-98.0)	- No hypoglycemia due to continuous infusion of glucose - Nausea (n = 14) and vomiting (n = 1)

malignant insulinomas often lack expression of GLP-1R but have high expression of SSTR.[16,52] This is reflected in various clinical imaging studies with exendin-4–based tracers, where false-negative cases were proven to be malignant insulinomas.[28,29,48,53] Interestingly, also differences in uptake between primary tumor and metastases[28,29] and uptake of both tracers in one lesion[43] were observed, stressing the variability in molecular phenotype of insulinomas, which should be taking into account when selecting the appropriate tracer. To be able to detect both benign and malignant lesions with one imaging procedure, a hybrid Lys^{27}([^{99m}Tc]Tc-EDDA/HYNIC)-exendin$^{9-39}$/[^{99m}Tc]Tc-EDDA/HYNIC-Tyr^3-octreotide formulation was prepared for simultaneous imaging of SSTR and GLP-1R.[54] Uptake of this tracer in SSTR and GLP-1R positive AR42J tumor xenografts was observed, and specificity for both targets was confirmed with blocking studies. In clinical practice, GLP-1R and SSTR

expression cannot be distinguished on the SPECT scan; however, evidence of local invasiveness and lymph node or liver metastases is indicative of malignant disease.[55] Alternatively, octreotide and exendin-4 in the hybrid tracer could be labeled with different radionuclides, enabling dual-radioisotope imaging.

3.3 | Prevent GLP-1R stimulation; reduction of peptide dose and use of receptor antagonists

Exendin-4 is a GLP-1R agonist and can therefore induce hypoglycemia because of receptor stimulation. GLP-1R agonists can induce insulin secretion, but this is dependent on elevated blood glucose levels, especially when levels exceed euglycemic concentrations of glucose. The effect of exendin-4 is thus self-regulating, and this lowers the risk of hypoglycemic events.[56] Other known side effects that may occur are nausea and vomiting. It is therefore important to minimize the peptide dose that is injected into patients, and various efforts have been made to increase specific activity. Christ et al first performed clinical SPECT imaging using a peptide dose of 30 μg, whereas in later clinical studies, doses of approximately 2 to 17 μg were used and also higher specific activities were achieved.[28,29,45-48,52] For PET imaging studies, peptide doses of 7 to 25 μg were injected, in which a wide range in peptide dose can be observed within and between studies.[40,41,43-46,53,57,58] Most studies using SPECT tracers did not report side effects like hypoglycemia, nausea, or vomiting.[28,29,48,52] However, in two studies where a SPECT tracer was administered, a substantial number of side effects (nausea and vomiting) were observed.[45,46] Clinical studies with exendin-based PET tracers led to only few cases of vomiting while more cases of nausea were reported.[40,41,43-46,53,57,58] Despite that the effect of exendin-4 is self-limiting,[56] there is still a substantial risk of hypoglycemia because of insulin release by functional insulinomas. In various studies, hypoglycemia was countered by glucose infusion or prevented by prophylactic glucose infusion. Blood glucose monitoring of patients is therefore essential once the tracer has been administered. The available data show that the occurrence of side effects was lower in studies with PET imaging compared with SPECT imaging, but this can depend on factors such as peptide dose and glucose infusion. For an overview of the clinical studies and tracers, see Tables 2 and 4.

Furthermore, studies have compared the use of exendin-4 with the receptor antagonist, exendin(9-39). Waser and Reubi showed excellent binding affinities in a Rip1Tag2 mouse model for both the agonist and antagonist.[59] Interestingly, Brom et al found that receptor affinity on INS-1 cells was high for both the agonist and antagonist, but the antagonist did not show internalization, and the tumor uptake was low.[60] The discrepancy between the studies can be explained by the receptor density, where the Rip1Tag2 mouse model has a higher number of receptors that can be bound by the antagonist. The number of bound receptors was not significantly different for the agonist and antagonist in case of the INS-1 cells.[60] Furthermore, when comparing the number of receptors for INS-1 cells and human insulinoma tissue, a substantial lower receptor density for human functioning insulinomas can be observed.[16,60] In case of a lower number of receptors, which is the situation in vivo, the agonist performs much better than the antagonist. Therefore, only the agonist is suitable for in vivo targeting of the GLP-1R.

Finally, several studies report on the use of radioiodinated antagonist-based tracers. [^{125}I]I-BH-exendin(9-39) exhibited high uptake in murine pancreas,[61] and the antagonist [Lys^{27}(^{125}I)I-BH-exendin(9-39)NH$_2$ demonstrated tumor uptake that was comparable with the agonists but with a substantially reduced kidney uptake.[51] In contrast, the antagonist [Nle^{14},[^{125}I]I-Tyr^{40}-NH$_2$]exendin(9-39) showed lower affinity and lower internalization than the more favorable agonist [Nle^{14},[^{125}I]I-Tyr^{40}-NH$_2$]exendin-4.[50]

3.4 | Fluorescence imaging for intraoperative detection of insulinoma

Because of the large penetration depth of γ-photons, whole-body imaging with SPECT and PET gives preoperative information on tumor size and location. Intraoperatively, gamma probes can be used for radioguided detection of tumors, as has been proven successful for [^{111}In]In-DOTA-exendin-4 for up to 14 days after tracer injection.[47] Fluorescence imaging probes provide images with better spatial resolution, and could therefore be used for more precise intraoperative delineation of the tumor, and fluorescence-guided surgery (FGS). Hypothetically, this will prevent unnecessary damage of pancreatic tissue, reduce the time that patients are under anesthesia, and related comorbidity. Various fluorescent exendin tracers have been developed,[62-66] with the primary goal of pancreatic beta cell visualization and quantification, although these are not used clinically so far. For in vivo imaging, fluorophores in the far-red wavelength (800 nm) are most suitable, since there is reduced autofluorescence of tissue at this wavelength, and because there is higher tissue penetration of 800-nm light. A frequently used dye for fluorescence guiding purposes is IRDye800CW, which has been conjugated to multiple targeting moieties and is increasingly used for clinical FGS in various solid tumor types.[67-69] We have developed a clinical grade exendin-4-IRDye800CW conjugate and shown

feasibility of insulinoma targeting and imaging in mice with subcutaneous GLP-1R overexpressing Chinese hamster lung cell tumors.[70] We intent to start clinical trials in which this tracer is employed for FGS of insulinoma. To combine high resolution, high sensitivity, and deep tissue penetration, dual-labeled targeting moieties with a radionuclide and fluorophore have been developed for other theranostic applications in oncology. One example is the carbonic anhydrase IX targeting probe [^{111}In]In-DTPA-G250-IRDye800CW for which fluorescence imaging was proven to be safe and suitable for intraoperative guidance of renal cell cancer resection in the clinic.[69] To the best of our knowledge, only Brand et al developed a dual-labeled exendin-4 tracer (fluorescein and ^{64}Cu).[71] With this tracer, small insulinoma xenografts were visualized with PET, and with fluorescence, individual pancreatic islets could be detected. Especially when conjugated with far-red fluorophores such as IRDye800CW, similar dual-modal tracers could be used for preoperative detection and intraoperative surgical guidance, ensuring complete resection of the insulinoma while preserving healthy pancreatic tissue.

4 | THERAPY WITH EXENDIN-4–BASED TRACERS

4.1 | Peptide receptor radionuclide therapy

Importantly, since for benign insulinoma surgical resection remains the therapy of choice, only patients with metastasized malignant insulinoma are eligible for (SSTR directed) PRRT. However, some effort has also been taken to develop exendin-4–based tracers for PRRT. As described above, ^{111}In-labeled exendin-4 analogs are predominantly used for imaging of γ-radiation, but indium-111 also emits low energy Auger electrons, which have a tissue penetration of only 0.02 µM to 10 µM. They exert their cytotoxic potential when in close proximity to the DNA after internalization. Auger electron emitting [Lys[40](Ahx-DTPA-[^{111}In]In)NH$_2$-exendin-4 efficiently repressed insulinoma growth in the Rip1Tag2 mouse model, but administration of high doses resulted in significant renal radiation damage and chronic renal failure.[72] Since all exendin-4–based tracers show high kidney uptake, kidney toxicity is a serious concern and precludes PRRT from clinical application at the moment.

4.2 | Kidney dosimetry and methods to reduce kidney uptake of exendin-4–based tracers

Some dosimetry studies have been performed with exendin-4–based tracers. Absorbed kidney doses that were found in case of exendin-4–based imaging tracers ranged from 0.1 to 4.5 mGy/MBq; these data were mostly derived from animal studies.[27,35,73,74] Furthermore, two studies investigated the potential of PRRT with ^{177}Lu-labeled exendin-4 using dosimetric calculations either extrapolated from biodistribution data of ^{177}Lu-labeled exendin-4 in rats or with a macro- and small-scale-dosimetry model[75] applied to ^{111}In-labeled exendin-4 SPECT/CT scans in humans.[73,76]

Estimated activities that could be administered without exceeding the maximum allowed absorbed kidney dose of 23 Gy were 3.8 GBq and 1.0 to 1.8 GBq, respectively. Concomitant absorbed insulinoma doses of 30 to 128 mGy/MBq were found, and these doses can lead to tumor shrinkage as was seen for pancreatic NETs after ^{177}Lu-labeled DOTATATE treatment.[77] Furthermore, the dose to the islets remained below 5 Gy, a dose which is considered a low risk of developing diabetes.[78] However, the absorbed kidney doses would allow for only one therapeutic cycle, in contrast to treatment with ^{177}Lu-labeled somatostatin analogs in which two to six cycles of 7.4 GBq are possible.[77] Higher injected doses and thus improved feasibility of PRRT with ^{177}Lu-labeled exendin-4 could be achieved by successfully lowering the renal accumulation.

Commonly used methods to reduce kidney uptake of peptide-based tracers are competitive inhibition of reabsorption by coinfusion of positively charged amino acids, trypsinized albumin, or the plasma expander gelofusine. Coinfusion of the combination of poly-glutamic acid and gelofusine has reduced renal uptake of ^{111}In-labeled exendin-4 by 48% in preclinical models.[79] Poly-glutamic acid is however not clinically available while gelofusine can be used in the clinical setting. In healthy volunteers, coinfusion of gelofusine showed a reduction of 18% in renal accumulation of ^{111}In-labeled exendin-4, without lowering tracer uptake in the pancreas.[76] Dosimetric calculations indicated that coinfusion with gelofusine increased the estimated allowable injected dose of ^{177}Lu-labeled exendin-4 with more than 20%, which would lead to higher absorbed insulinoma doses.

Other strategies to reduce renal uptake are introduction of a cleavable linker to allow renal excretion of the radionuclides,[80] inhibition of neutral endopeptidases to increase metabolic stability of the peptide in the circulation,[79,81-84] and incorporation of highly lipophilic groups[34] (efficacies of these strategies are summarized in Table 5). Furthermore, groups have conjugated exendin to PEG,[85-87] albumin,[88] an albumin binding domain,[89] a nonglycosylated human Fc fragment,[90] or nanoparticles[91-93] to increase circulation time. Since these strategies potentially increase uptake of the exendin-4 conjugates in other organs such as the liver, biodistribution and potency for imaging should be assessed for every compound.

TABLE 5 Strategies to lower kidney uptake of exendin-4–based tracers and their efficacy as described in various studies

Strategy	Outcome
Cleavable linker	• No significant change in kidney retention in comparison with [^{111}In]In-Ex4NOD40. It was assumed that the peptides were not cleaved before reabsorption in vivo.[80]
Inhibition of neutral endopeptidases	• Polygelines Haemaccel and gelofusine both increased urinary secretion of protein β_2-microglobulin, most likely explained by competitive inhibition of tubular protein reabsorption.[81] • Gelofusine and poly-glutamic acid (PGA) reduced kidney uptake by 18.7% and 29.4%, respectively. Gelofusine and PGA combined decreased kidney uptake by 47.9%.[79] • Gelofusine, albumin fragments, and lysine decreased renal uptake by 52%, 25%, and 15%, respectively.[82] • Albumin-derived peptide lowered renal uptake by 26% while gelofusine led to a reduction of 16%.[84]
Incorporation of highly lipophilic groups	• Kidney uptake was considerably lower compared with radiometal-labeled compounds and ranged from 30 to 50 %ID/g.[34]

Clinical applicability of exendin-4–based PRRT thus depends on multiple factors. First, renal accumulation should be largely reduced using improved or novel strategies to allow for higher insulinoma doses and possibly enable multiple therapy cycles. Another important factor using exendin-4 for PRRT is achieving a high specific activity, which enables the injection of therapeutic activity doses while keeping peptide doses sufficiently low. Low specific activities require the administration of higher peptide doses and could increase the risk of side effects. Preferably, peptide doses should be comparable with doses applied in imaging; nevertheless, the risk of side effects should be evaluated carefully.

4.3 | Photodynamic therapy

To avoid kidney toxicity, photodynamic therapy (PDT) might be an alternative tumor-ablative intervention. PDT involves administration of a photosensitizer (PS), followed by specific illumination of the tumor with light of a specific wavelength, often in the near infrared (NIR) range.[94] The activated PS will be converted from the ground singlet energy state into the excited singlet state. The PS can then decay back to the ground state, thereby emitting fluorescence, or it can undergo intersystem crossing and go to an excited triplet state. In this state, it can react directly with a substrate, which then reacts with oxygen to produce oxygenated products, or it can react directly with oxygen to form $^1O_2$.[94] Products of these two reactions are responsible for cell killing.[95] A large number of PSs have been developed and tested for treatment of cancer.[96] First generation porphyrin-based PSs were effectively used for treatment of various cancers, such as melanoma[97]; however, they were also taken up in normal tissue and skin, leading to severe skin phototoxicity. Hypericin is a second-generation PS that was shown to effectively internalize and accumulate in RINm5F insulinoma cells, and upon illumination, it induced apoptosis[98]; however, no experiments in in vivo models have been described so far.

By conjugating a PS to a tumor targeting molecule, it is possible to induce very specific cell death of target-expressing cells, a concept referred to as targeted photodynamic therapy (tPDT)[99] (Figure 1). This strategy will decrease side effects caused by accumulation of PSs in normal tissues. The technique is increasingly applied in various types of cancer, and a first clinical trial with cetuximab conjugated to the PS IRDye700DX in head-and-neck cancer patients is currently performed (ClinicalTrials.gov identifier NCT02422979). IRDye700DX is a frequently used PS in tPDT applications, mainly because of its high quantum yield, favorable excitation characteristics, and hydrophilicity of the molecule. Exendin-based tPDT could be a future application for ablation of small tumors in the pancreas, thereby reducing morbidity caused by unneeded radical resections. Furthermore, inoperable tumors that are in the near vicinity of, eg, the pancreatic duct could be removed without damaging these vital structures. These procedures could be performed laparoscopically since lasers for PDT are clinically available. We have developed an exendin-4-IRDye700DX conjugate, which causes very efficient and specific cell death of GLP-1R expressing cells in vitro and in vivo.[100]

5 | FUTURE OUTLOOK ON THE USE OF EXENDIN-4 IN INSULINOMA THERANOSTICS

SPECT and PET imaging with exendin-4 analogs provide means for delineation and localization of insulinoma lesions. Compared with SPECT, PET imaging is preferable because of increased spatial resolution and therefore better tumor delineation. Currently, gallium-68 is the most universally available and affordable positron emitter, offering easy labeling via a chelator. The sensitivity of [^{68}Ga]Ga-DOTA-exendin-4 PET/CT has proven to be superior to the sensitivity of [^{111}In]In-DTPA-exendin-4 SPECT/CT or MRI.[46] When NODAGA is used instead of DOTA, a higher
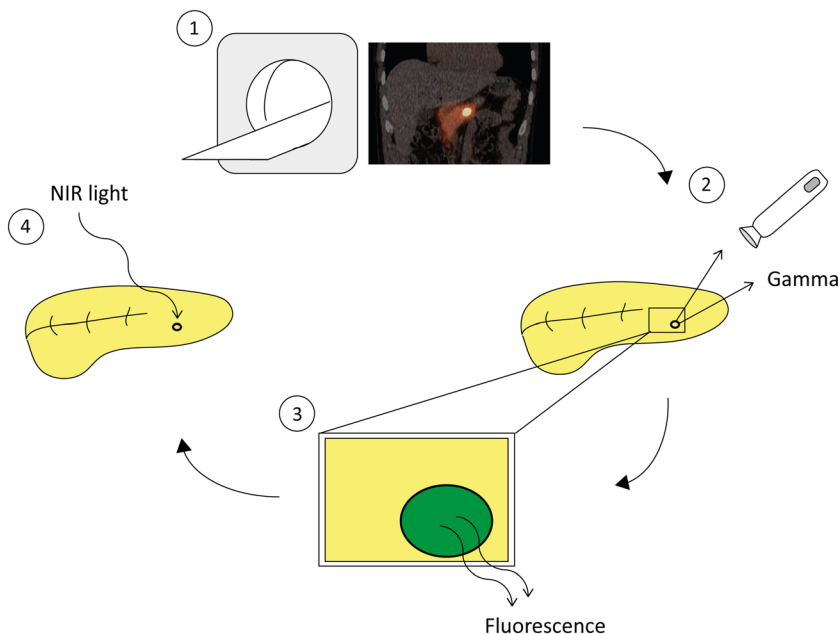
FIGURE 2 Multimodal exendin for theranostics of insulinoma. Radiolabeled exendin-4 can be used for SPECT or PET imaging to locate the lesion (1), however to detect the lesion intraoperatively a gamma probe (2) and fluorescence imaging (3) can be used. Furthermore the lesion can then be treated with NIR light to eradicate GLP-1R expressing cells (4).

specific activity can be obtained, allowing administration of lower peptide doses and thus minimizing risk of side effects due to receptor activation.[101,102] Therefore, we are currently performing a prospective multicenter study comparing [^{68}Ga]Ga-NODAGA-exendin PET/CT with MRI and [^{68}Ga]Ga-DOTA-TATE PET/CT (ClinicalTrials.gov identifier NCT03189953).[101,102]

Upon localization of an insulinoma, surgical resection is the treatment of choice; however, this is not always possible because of risk of complications or inoperability of patients. Therefore, imaging methods could merge into theranostics when exendin-4 is also used as a tracer for PRRT or tPDT. Currently, radiotoxicity in other tissues that take up or excrete the exendin-4–based tracers limits application of PRRT.[73] tPDT could be used for specific elimination of tumor cells, without causing damage to other tissues. Importantly, compared with benign insulinomas, malignant insulinomas are known to have increased expression of SSTR and limited expression of GLP-1R. Therefore, assessment of expression of these targets by nuclear imaging would be essential before applying tracer-based therapy.

To conclude, because of superior sensitivity when compared with conventional imaging methods, we believe that exendin-4–based PET/CT imaging should be considered as a primary method in patients with biochemical signs of insulinoma, enabling a one-stop shop procedure for detection and localization of insulinoma. Surgery will remain the therapy of choice for benign insulinoma, since high kidney uptake precludes the use of exendin-4–based tracers for PRRT. However, exendin-4–based tracers conjugated to fluorescent molecules may enable FGS or specific elimination of

insulinomas with tPDT, without causing kidney damage (Figure 2).

ORCID

Tom.J.P. Jansen   https://orcid.org/0000-0002-6466-7838

REFERENCES

1. Valente LG, Antwi K, Nicolas GP, Wild D, Christ E. Clinical presentation of 54 patients with endogenous hyperinsulinaemic hypoglycaemia: a neurological chameleon (observational study). *Swiss Med Wkly*. 2018;148:w14682.

2. Dizon AM, Kowalyk S, Hoogwerf BJ. Neuroglycopenic and other symptoms in patients with insulinomas. *Am J Med*. 1999;106(3): 307-310.

3. Mehrabi A, Fischer L, Hafezi M, et al. A systematic review of localization, surgical treatment options, and outcome of insulinoma. *Pancreas*. 2014;43(5):675-686.

4. Okabayashi T, Shima Y, Sumiyoshi T, et al. Diagnosis and management of insulinoma. *World J Gastroenterol*. 2013;19(6): 829-837.

5. Oberg K. Management of functional neuroendocrine tumors of the pancreas. *Gland Surg*. 2018;7(1):20-27.

6. Davi MV, Pia A, Guarnotta V, et al. The treatment of hyperinsulinemic hypoglycaemia in adults: an update. *J Endocrinol Invest*. 2017;40(1):9-20.

7. Kinova MK. Diagnostics and treatment of insulinoma. *Neoplasma*. 2015;62(5):692-704.

8. Service FJ, McMahon MM, O'Brien PC, Ballard DJ. Functioning insulinoma—incidence, recurrence, and long-term survival of patients: a 60-year study. *Mayo Clin Proc.* 1991;66(7):711-719.

9. Guettier JM, Kam A, Chang R, et al. Localization of insulinomas to regions of the pancreas by intraarterial calcium stimulation: the NIH experience. *J Clin Endocrinol Metab.* 2009;94(4):1074-1080.

10. Druce MR, Muthuppalaniappan VM, O'Leary B, et al. Diagnosis and localisation of insulinoma: the value of modern magnetic resonance imaging in conjunction with calcium stimulation catheterisation. *Eur J Endocrinol.* 2010;162(5):971-978.

11. Mossman AK, Pattison DA, Hicks RJ, Hamblin PS, Yates CJ. Localisation of occult extra-pancreatic insulinoma using glucagon-like peptide-1 receptor molecular imaging. *Intern Med J.* 2018;48(1):97-98.

12. Rayamajhi SJ, Lee J, Mittal BR, Jessop AC, Chasen B, Bhosale P. Cross sectional and nuclear medicine imaging of pancreatic insulinomas. *Abdom Radiol (NY).* 2017;42(2):531-543.

13. Lamberts SW, Bakker WH, Reubi JC, Krenning EP. Somatostatin receptor imaging in vivo localization of tumors with a radiolabeled somatostatin analog. *J Steroid Biochem Mol Biol.* 1990;37(6):1079-1082.

14. Lamberts SW, Bakker WH, Reubi JC, Krenning EP. Somatostatin-receptor imaging in the localization of endocrine tumors. *N Engl J Med.* 1990;323(18):1246-1249.

15. Zimmer T, Stolzel U, Bader M, et al. Endoscopic ultrasonography and somatostatin receptor scintigraphy in the preoperative localisation of insulinomas and gastrinomas. *Gut.* 1996;39(4):562-568.

16. Reubi JC, Waser B. Concomitant expression of several peptide receptors in neuroendocrine tumours: molecular basis for in vivo multireceptor tumour targeting. *Eur J Nucl Med Mol I.* 2003;30(5):781-793.

17. Prasad V, Sainz-Esteban A, Arsenic R, et al. Role of (68)Ga somatostatin receptor PET/CT in the detection of endogenous hyperinsulinaemic focus: an explorative study. *Eur J Nucl Med Mol Imaging.* 2016;43(9):1593-1600.

18. Sadowski SM, Neychev V, Cottle-Delisle C, et al. Detection of insulinoma using (68)Gallium-DOTATATE PET/CT: a case report. *Gland Surg.* 2014;3(4):E1-E5.

19. Reubi JC, Waser B. Concomitant expression of several peptide receptors in neuroendocrine tumours: molecular basis for in vivo multireceptor tumour targeting. *Eur J Nucl Med Mol Imaging.* 2003;30(5):781-793.

20. Gotthardt M, Fischer M, Naeher I, et al. Use of the incretin hormone glucagon-like peptide-1 (GLP-1) for the detection of insulinomas: initial experimental results. *Eur J Nucl Med Mol Imaging.* 2002;29(5):597-606.

21. Eng J, Kleinman WA, Singh L, Singh G, Raufman JP. Isolation and characterization of exendin-4, an exendin-3 analogue, from *Heloderma suspectum* venom. Further evidence for an exendin receptor on dispersed acini from guinea pig pancreas. *J Biol Chem.* 1992;267(11):7402-7405.

22. Deacon CF, Knudsen LB, Madsen K, Wiberg FC, Jacobsen O, Holst JJ. Dipeptidyl peptidase IV resistant analogues of glucagon-like peptide-1 which have extended metabolic stability and improved biological activity. *Diabetologia.* 1998;41(3):271-278.

23. Gotthardt M, Lalyko G, van Eerd-Vismale J, et al. A new technique for in vivo imaging of specific GLP-1 binding sites: first results in small rodents. *Regul Pept.* 2006;137(3):162-167.

24. Wild D, Behe M, Wicki A, et al. [Lys40(Ahx-DTPA-111In)NH2]exendin-4, a very promising ligand for glucagon-like peptide-1 (GLP-1) receptor targeting. *J Nucl Med.* 2006;47(12):2025-2033.

25. Wild D, Macke H, Christ E, Gloor B, Reubi JC. Glucagon-like peptide 1-receptor scans to localize occult insulinomas. *N Engl J Med.* 2008;359(7):766-768.

26. Christ E, Wild D, Ederer S, et al. Glucagon-like peptide-1 receptor imaging for the localisation of insulinomas: a prospective multicentre imaging study. *Lancet Diabetes Endocrinology.* 2013;1(2):115-122.

27. Wild D, Wicki A, Mansi R, et al. Exendin-4-based radiopharmaceuticals for glucagonlike peptide-1 receptor PET/CT and SPECT/CT. *J Nucl Med.* 2010;51(7):1059-1067.

28. Sowa-Staszczak A, Pach D, Mikolajczak R, et al. Glucagon-like peptide-1 receptor imaging with [Lys40(Ahx-HYNIC-99mTc/EDDA)NH2]-exendin-4 for the detection of insulinoma. *Eur J Nucl Med Mol Imaging.* 2013;40(4):524-531.

29. Sowa-Staszczak A, Trofimiuk-Muldner M, Stefanska A, et al. 99mTc labeled glucagon-like peptide-1-analogue (99mTc-GLP1) scintigraphy in the management of patients with occult insulinoma. *PLoS ONE.* 2016;11(8):e0160714.

30. Kiesewetter DO, Gao H, Ma Y, et al. 18F-radiolabeled analogs of exendin-4 for PET imaging of GLP-1 in insulinoma. *Eur J Nucl Med Mol Imaging.* 2012;39(3):463-473.

31. Yue X, Kiesewetter DO, Guo J, et al. Development of a new thiol site-specific prosthetic group and its conjugation with [Cys(40)]-exendin-4 for in vivo targeting of insulinomas. *Bioconjug Chem.* 2013;24(7):1191-1200.

32. Wu H, Liang S, Liu S, Pan Y, Cheng D, Zhang Y. 18F-radiolabeled GLP-1 analog exendin-4 for PET/CT imaging of insulinoma in small animals. *Nucl Med Commun.* 2013;34(7):701-708.

33. Wu Z, Liu S, Hassink M, et al. Development and evaluation of 18F-TTCO-Cys40-exendin-4: a PET probe for imaging transplanted islets. *J Nucl Med.* 2013;54(2):244-251.

34. Dialer LO, Jodal A, Schibli R, Ametamey SM, Behe M. Radiosynthesis and evaluation of an (18)F-labeled silicon containing exendin-4 peptide as a PET probe for imaging insulinoma. *EJNMMI Radiopharm Chem.* 2018;3(1):1.

35. Mikkola K, Yim CB, Lehtiniemi P, et al. Low kidney uptake of GLP-1R-targeting, beta cell-specific PET tracer, (18)F-labeled [Nle(14),Lys(40)]exendin-4 analog, shows promise for clinical imaging. *EJNMMI Res.* 2016;6(1):91.

36. Kiesewetter DO, Guo N, Guo J, et al. Evaluation of an [(18)F]AlF-NOTA analog of exendin-4 for imaging of GLP-1 receptor in insulinoma. *Theranostics.* 2012;2(10):999-1009.

37. Xu Q, Zhu C, Xu Y, et al. Preliminary evaluation of [18F]AlF-NOTA-MAL-Cys39-exendin-4 in insulinoma with PET. *J Drug Target.* 2015;23(9):813-820.

38. Xu Y, Pan D, Xu Q, et al. Insulinoma imaging with glucagon-like peptide-1 receptor targeting probe (18)F-FBEM-Cys (39)-exendin-4. *J Cancer Res Clin Oncol*. 2014;140(9):1479-1488.

39. Selvaraju RK, Velikyan I, Asplund V, et al. Pre-clinical evaluation of [(68)Ga]Ga-DO3A-VS-Cys(40)-exendin-4 for imaging of insulinoma. *Nucl Med Biol*. 2014;41(6):471-476.

40. Eriksson O, Velikyan I, Selvaraju RK, et al. Detection of metastatic insulinoma by positron emission tomography with [(68)Ga]exendin-4-a case report. *J Clin Endocrinol Metab*. 2014;99(5):1519-1524.

41. Luo Y, Yu M, Pan Q, et al. ^{68}Ga-NOTA-exendin-4 PET/CT in detection of occult insulinoma and evaluation of physiological uptake. *Eur J Nucl Med Mol Imaging*. 2015;42(3):531-532.

42. Cuthbertson DJ, Banks M, Khoo B, et al. Application of Ga(68)-DOTA-exendin-4 PET/CT to localize an occult insulinoma. *Clin Endocrinol (Oxf)*. 2016;84(5):789-791.

43. Luo Y, Pan Q, Yao S, et al. Glucagon-like peptide-1 receptor PET/CT with ^{68}Ga-NOTA-exendin-4 for detecting localized insulinoma: a prospective cohort study. *J Nucl Med*. 2016;57(5):715-720.

44. Parihar AS, Vadi SK, Kumar R, et al. [68]Ga DOTA-exendin PET/CT for detection of insulinoma in a patient with persistent hyperinsulinemic hypoglycemia. *Clin Nucl Med*. 2018;43(8):e285-e286.

45. Antwi K, Fani M, Nicolas G, et al. Localization of hidden insulinomas with (6)(8)Ga-DOTA-exendin-4 PET/CT: a pilot study. *J Nucl Med*. 2015;56(7):1075-1078.

46. Antwi K, Fani M, Heye T, et al. Comparison of glucagon-like peptide-1 receptor (GLP-1R) PET/CT, SPECT/CT and 3T MRI for the localisation of occult insulinomas: evaluation of diagnostic accuracy in a prospective crossover imaging study. *Eur J Nucl Med Mol Imaging*. 2018;45(13):2318-2327.

47. Christ E, Wild D, Forrer F, et al. Glucagon-like peptide-1 receptor imaging for localization of insulinomas. *J Clin Endocrinol Metab*. 2009;94(11):4398-4405.

48. Christ E, Wild D, Ederer S, et al. Glucagon-like peptide-1 receptor imaging for the localisation of insulinomas: a prospective multicentre imaging study. *Lancet Diabetes Endocrinology*. 2013;1(2):115-122.

49. Bauman A, Valverde IE, Fischer CA, Vomstein S, Mindt TL. Development of [68]Ga- and [89]Zr-labeled exendin-4 as potential radiotracers for the imaging of insulinomas by PET. *J Nucl Med*. 2015;56(10):1569-1574.

50. Lappchen T, Tonnesmann R, Eersels J, Meyer PT, Maecke HR, Rylova SN. Radioiodinated exendin-4 is superior to the radiometal-labelled glucagon-like peptide-1 receptor probes overcoming their high kidney uptake. *PLoS ONE*. 2017;12(1):e0170435.

51. Rylova SN, Waser B, Del Pozzo L, et al. Approaches to improve the pharmacokinetics of radiolabeled glucagon-like peptide-1 receptor ligands using antagonistic tracers. *J Nucl Med*. 2016;57(8):1282-1288.

52. Wild D, Christ E, Caplin ME, et al. Glucagon-like peptide-1 versus somatostatin receptor targeting reveals 2 distinct forms of malignant insulinomas. *J Nucl Med*. 2011;52(7):1073-1078.

53. Bongetti E, Lee MH, Pattison DA, et al. Diagnostic challenges in a patient with an occult insulinoma:(68)Ga-DOTA-exendin-4 PET/CT and (68)Ga-DOTATATE PET/CT. *Clin Case Rep*. 2018;6(4):719-722.

54. Medina-Garcia V, Ocampo-Garcia BE, Ferro-Flores G, et al. A freeze-dried kit formulation for the preparation of Lys(27) ([99]mTc-EDDA/HYNIC)-exendin(9-39)/[99]mTc-EDDA/HYNIC-Tyr3-octreotide to detect benign and malignant insulinomas. *Nucl Med Biol*. 2015;42(12):911-916.

55. Grant CS. Insulinoma. *Best Pract Res Clin Gastroenterol*. 2005;19(5):783-798.

56. Meloni AR, DeYoung MB, Lowe C, Parkes DG. GLP-1 receptor activated insulin secretion from pancreatic beta-cells: mechanism and glucose dependence. *Diabetes Obes Metab*. 2013;15(1):15-27.

57. Luo Y, Li J, Yang A, Yang H, Li F. ^{68}Ga-exendin-4 PET/CT in evaluation of endoscopic ultrasound-guided ethanol ablation of an insulinoma. *Clin Nucl Med*. 2017;42(4):310-311.

58. Luo Y, Li N, Kiesewetter DO, Chen X, Li F. ^{68}Ga-NOTA-exendin-4 PET/CT in localization of an occult insulinoma and appearance of coexisting esophageal carcinoma. *Clin Nucl Med*. 2016;41(4):341-343.

59. Waser B, Reubi JC. Value of the radiolabelled GLP-1 receptor antagonist exendin(9-39) for targeting of GLP-1 receptor-expressing pancreatic tissues in mice and humans. *Eur J Nucl Med Mol Imaging*. 2011;38(6):1054-1058.

60. Brom M, Joosten L, Oyen WJ, Gotthardt M, Boerman OC. Radiolabelled GLP-1 analogues for in vivo targeting of insulinomas. *Contrast Media Mol Imaging*. 2012;7(2):160-166.

61. Mukai E, Toyoda K, Kimura H, et al. GLP-1 receptor antagonist as a potential probe for pancreatic beta-cell imaging. *Biochem Biophys Res Commun*. 2009;389(3):523-526.

62. Lehtonen J, Schaffer L, Rasch MG, Hecksher-Sorensen J, Ahnfelt-Ronne J. Beta cell specific probing with fluorescent exendin-4 is progressively reduced in type 2 diabetic mouse models. *Islets*. 2015;7(6):e1137415.

63. Reiner T, Thurber G, Gaglia J, et al. Accurate measurement of pancreatic islet beta-cell mass using a second-generation fluorescent exendin-4 analog. *Proc Natl Acad Sci U S A*. 2011;108(31):12815-12820.

64. Kirkpatrick A, Heo J, Abrol R, Goddard WA 3rd. Predicted structure of agonist-bound glucagon-like peptide 1 receptor, a class B G protein-coupled receptor. *Proc Natl Acad Sci U S A*. 2012;109(49):19988-19993.

65. Clardy SM, Keliher EJ, Mohan JF, et al. Fluorescent exendin-4 derivatives for pancreatic beta-cell analysis. *Bioconjug Chem*. 2014;25(1):171-177.

66. Reiner T, Kohler RH, Liew CW, et al. Near-infrared fluorescent probe for imaging of pancreatic beta cells. *Bioconjug Chem*. 2010;21(7):1362-1368.

67. Gao RW, Teraphongphom N, de Boer E, et al. Safety of panitumumab-IRDye800CW and cetuximab-IRDye800CW for fluorescence-guided surgical navigation in head and neck cancers. *Theranostics*. 2018;8(9):2488-2495.

68. Li D, Zhang J, Chi C, et al. First-in-human study of PET and optical dual-modality image-guided surgery in glioblastoma using (68)Ga-IRDye800CW-BBN. *Theranostics*. 2018;8(9):2508-2520.

69. Hekman MC, Rijpkema M, Muselaers CH, et al. Tumor-targeted dual-modality imaging to improve intraoperative

visualization of clear cell renal cell carcinoma: a first in man study. *Theranostics*. 2018;8(8):2161-2170.

70. Boss M, Buitinga M, Brom M, et al. Targeted optical imaging of the GLP-1R using exendin-IRDye800CW. *Eur J Nucl Med Mol I*. 2018;45:S76-S77.

71. Brand C, Abdel-Atti D, Zhang Y, et al. In vivo imaging of GLP-1R with a targeted bimodal PET/fluorescence imaging agent. *Bioconjug Chem*. 2014;25(7):1323-1330.

72. Wicki A, Wild D, Storch D, et al. [Lys40(Ahx-DTPA-111In)NH2]-exendin-4 is a highly efficient radiotherapeutic for glucagon-like peptide-1 receptor-targeted therapy for insulinoma. *Clin Cancer Res*. 2007;13(12):3696-3705.

73. Selvaraju RK, Bulenga TN, Espes D, et al. Dosimetry of [(68)Ga]Ga-DO3A-VS-Cys(40)-exendin-4 in rodents, pigs, non-human primates and human—repeated scanning in human is possible. *Am J Nucl Med Mol Imaging*. 2015;5(3):259-269.

74. Mikkola K, Yim CB, Fagerholm V, et al. ⁶⁴Cu- and ⁶⁸Ga-labelled [Nle(14),Lys(40)(Ahx-NODAGA)NH2]-exendin-4 for pancreatic beta cell imaging in rats. *Mol Imaging Biol*. 2014;16(2):255-263.

75. van der Kroon I, Woliner-van der Weg W, Brom M, et al. Whole organ and islet of Langerhans dosimetry for calculation of absorbed doses resulting from imaging with radiolabeled exendin. *Sci Rep*. 2017;7(1):39800.

76. Buitinga M, Jansen TJP, van der Kroon I, et al. Succinylated gelatin improves the theranostic potential of radiolabeled exendin-4 in insulinoma patients. *J Nucl Med*. 2018. jnumed.118.219980

77. Ilan E, Sandstrom M, Wassberg C, et al. Dose response of pancreatic neuroendocrine tumors treated with peptide receptor radionuclide therapy using 177Lu-DOTATATE. *J Nucl Med*. 2015;56(2):177-182.

78. de Vathaire F, El-Fayech C, Ben Ayed FF, et al. Radiation dose to the pancreas and risk of diabetes mellitus in childhood cancer survivors: a retrospective cohort study. *Lancet Oncol*. 2012;13(10):1002-1010.

79. Gotthardt M, van Eerd-Vismale J, Oyen WJG, et al. Indication for different mechanisms of kidney uptake of radiolabeled peptides. *J Nucl Med*. 2007;48(4):596-601.

80. Jodal A, Pape F, Becker-Pauly C, Maas O, Schibli R, Behe M. Evaluation of (1)(1)(1)in-labelled exendin-4 derivatives containing different meprin beta-specific cleavable linkers. *PLoS ONE*. 2015;10(4):e0123443.

81. Veldman BA, Schepkens HL, Vervoort G, Klasen I, Wetzels JF. Low concentrations of intravenous polygelines promote low-molecular weight proteinuria. *Eur J Clin Invest*. 2003;33(11):962-968.

82. Vegt E, van Eerd JE, Eek A, et al. Reducing renal uptake of radiolabeled peptides using albumin fragments. *J Nucl Med*. 2008;49(9):1506-1511.

83. Vegt E, de Jong M, Wetzels JF, et al. Renal toxicity of radiolabeled peptides and antibody fragments: mechanisms, impact on radionuclide therapy, and strategies for prevention. *J Nucl Med*. 2010;51(7):1049-1058.

84. Vegt E, Eek A, Oyen WJ, de Jong M, Gotthardt M, Boerman OC. Albumin-derived peptides efficiently reduce renal uptake of radiolabelled peptides. *Eur J Nucl Med Mol Imaging*. 2010;37(2):226-234.

85. Lee SH, Lee S, Youn YS, et al. Synthesis, characterization, and pharmacokinetic studies of PEGylated glucagon-like peptide-1. *Bioconjug Chem*. 2005;16(2):377-382.

86. Kim TH, Jiang HH, Lee S, et al. Mono-PEGylated dimeric exendin-4 as high receptor binding and long-acting conjugates for type 2 anti-diabetes therapeutics. *Bioconjug Chem*. 2011;22(4):625-632.

87. Babic A, Vinet L, Chellakudam V, Janikowska K, Allemann E, Lange N. Squalene-PEG-exendin as high-affinity constructs for pancreatic beta-cells. *Bioconjug Chem*. 2018;29(8):2531-2540.

88. Baggio LL, Huang Q, Brown TJ, Drucker DJ. A recombinant human glucagon-like peptide (GLP)-1-albumin protein (albugon) mimics peptidergic activation of GLP-1 receptor-dependent pathways coupled with satiety, gastrointestinal motility, and glucose homeostasis. *Diabetes*. 2004;53(9):2492-2500.

89. O'Connor-Semmes RL, Lin J, Hodge RJ, et al. GSK2374697, a novel albumin-binding domain antibody (AlbudAb), extends systemic exposure of exendin-4: first study in humans—PK/PD and safety. *Clin Pharmacol Ther*. 2014;96(6):704-712.

90. Choi IY, Park SH, Lee KH, et al. A long-acting exendin-4 analog conjugate to the human Fc-fragment reveals low immunogenic potential. *Diabetes*. 2014;63:A259-A260.

91. Zhang B, Yang B, Zhai C, Jiang B, Wu Y. The role of exendin-4-conjugated superparamagnetic iron oxide nanoparticles in beta-cell-targeted MRI. *Biomaterials*. 2013;34(23):5843-5852.

92. Chuang EY, Nguyen GT, Su FY, et al. Combination therapy via oral co-administration of insulin- and exendin-4-loaded nanoparticles to treat type 2 diabetic rats undergoing OGTT. *Biomaterials*. 2013;34(32):7994-8001.

93. Wang P, Yoo B, Yang J, et al. GLP-1R-targeting magnetic nanoparticles for pancreatic islet imaging. *Diabetes*. 2014;63(5):1465-1474.

94. Henderson BW, Dougherty TJ. How does photodynamic therapy work? *Photochem Photobiol*. 1992;55(1):145-157.

95. Moan J, Berg K. The photodegradation of porphyrins in cells can be used to estimate the lifetime of singlet oxygen. *Photochem Photobiol*. 1991;53(4):549-553.

96. Deng K, Li C, Huang S, et al. Recent progress in near infrared light triggered photodynamic therapy. *Small*. 2017;13(44).

97. Baldea I, Filip AG. Photodynamic therapy in melanoma—an update. *J Physiol Pharmacol*. 2012;63(2):109-118.

98. Yi J, Yang X, Zheng L, et al. Photoactivation of hypericin decreases the viability of RINm5F insulinoma cells through reduction in JNK/ERK phosphorylation and elevation of caspase-9/caspase-3 cleavage and Bax-to-Bcl-2 ratio. *Biosci Rep*. 2015;35(3):1-13.

99. Mitsunaga M, Ogawa M, Kosaka N, Rosenblum LT, Choyke PL, Kobayashi H. Cancer cell-selective in vivo near infrared photoimmunotherapy targeting specific membrane molecules. *Nat Med*. 2011;17(12):1685-1691.

100. Boss M, Brom M, Bos DL, et al. Targeted photodynamic therapy of GLP-1R positive lesions with exendin-IRDye700DX. *Eur J Nucl Med Mol I*. 2018;45:S166-S166.

101. Boss M, Mikkola K, Buitinga M, et al. Ga-68-NODAGA-exendin-4 PET/CT for the localization of insulinomas. *Eur J Nucl Med Mol I.* 2018;45:S87-S88.

102. Boss M, Buitinga M, Brom M, et al. ^{68}Ga-NODAGA-exendin-4 PET/CT for the localization of insulinomas: preliminary data from a prospective multicenter imaging study. *Neuroendocrinology.* 2017;105:165-165.

AUTHOR BIOGRAPHIES

Tom Jansen studied Technical Medicine at the University of Twente. After graduating in 2016, he started his PhD project at the Department of Radiology and Nuclear Medicine of the Radboudumc, Nijmegen. This project aims to further investigate type 1 diabetes, performing several clinical studies using GLP-1R imaging. Furthermore, this PhD project aims to improve research on type 1 diabetes, establishing collaborations within Europe through the international consortium INNODIA.

Sanne van Lith studied Biomedical Sciences at the Radboud University, Nijmegen. She graduated in 2012 and did her PhD project at the Department of Pathology of the Radboudumc, Nijmegen. In 2017 she started as a post-doc researcher at the department of Radiology and Nuclear Medicine of the Radboudumc. Her projects involve tracer development and implementation for imaging and photodynamic therapy in oncology.

Marti Boss studied Molecular Lifesciences at Maastricht University and Molecular and Cellular Lifesciences at Utrecht University, where she received her master's degree in 2010. After working as a technician at Crucell Holland BV (Johnson & Johnson) she started her PhD project at the Department of Nuclear Medicine at the Radboudumc in 2014. The main focus of her research over the last years has been on theranostics of hyperinsulinemic hypoglycaemia using radiolabeled as well as fluorescently labeled tracers encompassing pre-clinical as well as clinical research.

Maarten Brom studied Life Sciences at the Hogeschool Utrecht and Molecular Life Sciences at HAN University, Nijmegen. After graduating in 2006, he started his PhD project in 2007 at the department of Radiology and Nuclear medicine of the Radboudumc Nijmegen, involving development of radiotracers for determination of beta-cell mass. He continued working on these projects, and on clinical implementation of exendin-based tracers as a post-doc researcher and group leader. Currently he works as a project manager at Tracer Europe BV, Groningen.

Lieke Joosten studied Biomedical Science at the Fontys Hogeschool in Eindhoven, followed by the master Oncology at the Vrije Universiteit in Amsterdam. After graduating in 2008, she started working as a research technician at the department of Radiology and Nuclear Medicine of the Radboudumc, Nijmegen. While working as a senior research technician, she started her PhD in 2015. Her PhD research is focused on beta cell imaging; development of new tracers and improvement of already existing tracers for visualizing insulinomas and beta cells in diabetes.

Martin Béhé studied chemistry at the University of Basel followed a by PhD thesis in the field of radiolabeled peptides. He further worked in this field at the University Hospitals in Göttingen, Marburg and Freiburg. He was involved in the development of the radiolabeled Exendin analogues and was responsible for their translation to clinical application. Now he holds a group leader positionat Paul Scherrer Institut, Switzerland. Beside radiolabeled peptides for G-protein coupled receptor targeting he also works in the field of targeting protein structures in extracellular matrices.

Mijke Buitinga studied Technical Medicine at the University of Twente. She did her PhD project at the Department of Developmental Bioengineering at the University of Twente on the development of novel bioengineering strategies to treat type 1 diabetes. From 2014, she worked as a postdoc in the group of Prof. Gotthardt (Radboudumc, the Netherlands), focusing on the characterization of beta-cell tracers to visualize and quantify beta-cell mass in (pre)clinical settings. In 2018, she started as a postdoc at the Department of Clinical and Experimental Endocrinology at KU Leuven.

Martin Gotthardt studied Medicine in Marburg (Germany) and wrote his thesis on the metabolism of glucagon-like peptide 1. In 2005, he started to work as a nuclear medicine specialist at the Department of Radiology and Nuclear Medicine at the Radboudumc, Nijmegen and continued his work with radiolabeled tracers for in vivo imaging of beta cells. He has coordinated the EU projects BetaImage, BetaCure and BetaTrain. Under his supervision, exendin derivatives have been introduced in clinical research. Since 2011, he holds a full chair for Experimental Nuclear Medicine at the Radboud University Nijmegen and is Head of Nuclear Medicine Research.